COMPUTATIONAL MODEL OF SHORT PULSE LASER TARGET INTERACTIONS

J. Limpouch, A.A. Andreev[1] and L. Drška

Faculty of Nuclear Science and Physical Engineering, Czech Technical University
Břehová 7, 115 19 Prague, Czech Republic

[1] *Institute for Laser Physics, Vavilov State Optical Institute*
Birzhevaya line 12, Skt. Petersburg, Russia

Abstract

A complex self-sustained 1D hydrodynamics model of interactions of ultrashort laser pulses with solid targets has been developed. The main application of the model is the interpretation of experiments through the comparison of the code results with output of various types of diagnostics. It can be also used in search of optimum experimental conditions for certain proposed applications of such systems.

1. Introduction

The development of T^3 (terawatt table-top) lasers have opened up opportunities for extensive research of interactions of high intensity (I $\simeq 10^{14} - 10^{19}$ W/cm^2) short laser pulses ($\tau \simeq$ 100 fs - 1 ps) with solid targets. The physics of this system is considerably different from conventional interactions of longer pulses as due to a short time scale hydrodynamic motion is no longer a dominant factor and high density plasmas are produced. The non-linear character of interaction is very apparent and a considerable part of energy is transferred to a group of very fast particles. A detailed review of experimental results and theoretical methods used for description of interaction of short laser pulses with solid target is presented in paper [1].

2. Computational model

The dynamics of plasma is described via one fluid two temperature Lagrangian hydrocode with electron and ion thermal conductivities, both natural and artificial ion viscosities, and ponderomotive force impact on plasma motion. Laser absorption, energy transport by fast electrons and energy losses via bremsstrahlung and recombination emission are included. Very fine spatial grid with typically 200 - 500 cells is used to model the shape of the density profile in the expanding plasma in detail so that the laser fields may be calculated properly.

The populations of all charge states Z in plasma are described via set of atomic rate equations, including collisional ionization, radiative and three body recombination.

Maxwell's equations are solved in the presented model both for s- and p-polarized laser radiation. The method of numerical solving of Maxwell's equations in hot plasma, taking into account spatial dispersion and Landau damping, is described in [2]. Wavebreaking is described in a phenomenological way by introduction of an effective damping rate of plasma wave.

The acceleration of electrons at resonant absorption is treated in each time step via stationary electron diffusion [3] in the velocity space. Electrons are accelerated preferentially in direction to the underdense plasma. The energy of fast electrons matches the difference between the overall laser absorption and integrated local collisional absorption, so that energy conservation is maintained. A typical electron distribution function $f_{accel}(v)$ of the accelerated electrons at the vacuum side of the acceleration region is plotted in Fig. 1 at the maximum of laser pulse. We assume fast electrons only these electrons carrying the net increase in energy flux density. These energetic electrons are then reflected back from the plasma-vacuum boundary losing a fraction η_i of their energy, so that the integral energy lost by fast electrons is equal to the energy gained by the energetic ions.

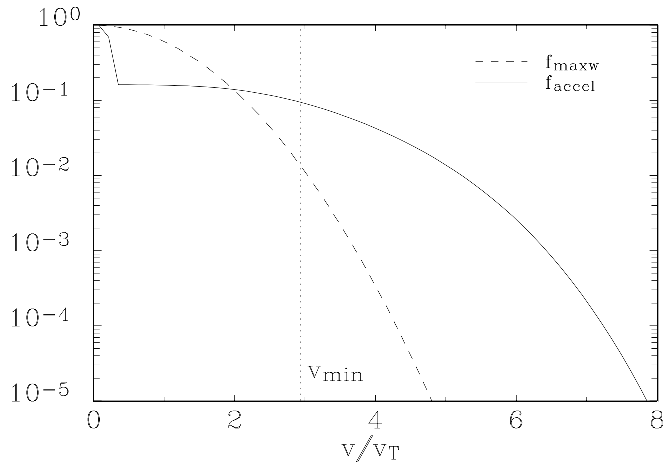

Fig. 1. Velocity spectrum f_{accel} of electrons accelerated by resonance absorption, f_{maxw} is the spectra of electrons incident from overdense plasma. Velocity v_{min} is the minimum velocity of the distribution function of fast electrons. The spectrum is taken at the maximum of p-polarized Gaussian 400 fs FWHM Nd-laser pulse with peak intensity 10^{16} W/cm^2 incident at 45° onto a solid aluminium target.

The distribution function of fast electrons reflected from plasma-vacuum boundary is then used as a boundary condition for solving the transport of energetic electrons into the solid target. The transport is described simply as continuous slowing down with the Bethe-Bloch stopping power. The time of flight of fast electrons inside the simulation box is neglected. The energy lost by fast electrons in a spatial cell leads to the heating of thermal electrons there.

Electrostatic acceleration of ions in the expanding plasma forming a double layer at the plasma-vacuum boundary is assumed. The spectrum of fast ions is found from the electron spectrum via model developed by Gurevich and Mescherkin [4]. This model assumes quasineutrality and the time of fast electron roundtrip in corona small compared to the laser pulse. Then the electron distribution is symmetric in longitudinal velocity v and electron concentration is given by an electrostatic potential. The evolution of ion density and velocity is then described by collisionless hydrodynamics. Ion velocity distribution is expressed via transformation of variables.

Second harmonics (SH) emission is a very important diagnostics tools which can provide a detailed information about particularly important region of critical surface neighbourhood. We have neglected the influence of SH fields back on the basic harmonics, which limits the range of validity of the model to medium laser intensities, where the energy conversion to SH is small. The phase of SH emission is controlled mainly by the motion of the source of SH emission which is near to critical surface and thus the shift of SH spectra near to the Doppler shift of radiation reflected from the moving critical surface.

Radiation transport in x-ray lines is modelled as a postprocessor to 1D hydrocode in planar geometry. The spectrum of K-shell line emission is calculated together with a self-consistent description of the excitation kinetics. In the implemented model for the simulation of non-equilibrium line transfer, the coupling is carried out by an iterative procedure, where the populations are obtained by linearization while the line transfer is computed within the core saturation approximation and with complete frequency redistribution [5]. Voigt emission and absorption line profiles are presently assumed, taking into account natural, lifetime, electron impact Stark and Doppler broadening. Macroscopic Doppler shift is taken into account on a Lagrangian hydrodynamic grid. Radiative transfer is solved together with the level populations only for potentially optically thick lines. As the transit time of radiation through plasma is negligible, radiative transfer is written in approximation of infinite speed of light.

3. Simulation results

Only a limited number of examples of simulation results can be shown here. First, the dependence of laser absorption and hot electron temperature on laser intensity is presented. Laser absorption efficiency, plotted in Fig. 2, decreases slowly with laser intensity. The increasing density profile modification due to increasing ponderomotive force leads not only to decrease of collisional absorption, but in our case also to a slight reduction of resonance absorption. However, for the highest intensity assumed here, the dynamics of plasma corona is very complicated, there are periods when plasma density profile changes rapidly and cavitons are formed. In this case a significant dependence of the overall absorption efficiency on the detailed parameters of simulations is observed. This uncertainty in absorption efficiency is represented by error bars in Fig. 2.

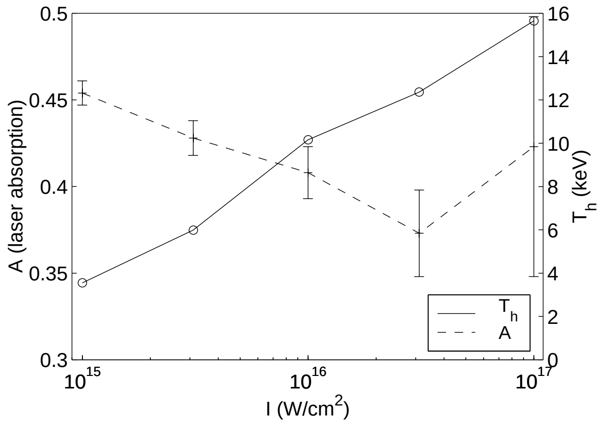

Fig. 2. Laser absorption efficiency A and hot electron temperature T_h versus laser intensity. P-polarized Nd laser 1.5 ps FWHM Gaussian pulse is incident at 45° on solid Al target.

Absorption efficiencies in our simulations are somewhat lower compared with experiments and some results of PIC code, see review paper [1]. The same figure depicts the rise of hot electron temperature with laser intensity. The deduced hot electron temperature is $T_h \sim I^\alpha$, where $\alpha \simeq 0.6$, which is in good agreement with scaling PIC simulations [6].

We present the calculations for the conditions of recent experiments [7]. Here, 1.5 ps FWHM pulse of p-polarized Nd-laser radiation was incident at 45^o onto plane Al target. Laser intensity was varied between 10^{16} and 10^{17} W/cm^2, intensity contrast was $\sim 10^6 - 10^7$. The fast ion spectrum was measured in direction normal to the target. The ion spectrum is presented for the respective intensities in Fig. 3. As the experimental spectrum is not absolutely calibrated, i.e. the total energy of fast ions is not known, the experimental spectrum is normalized, so that the maxima of fast ion distributions are equal. An excellent agreement with measurement in fast ion energy and spectrum is obtained.

The overall efficiency of energy transformation to SH emission is plotted in Fig. 4 versus laser peak intensity. The experimental results are plotted together with the theoretical fit

$\eta = I_2/I_0 \sim I_0$. This dependence is obtained, when resonance absorption is linear and plasma parameters and the density profile do not vary with the laser intensity. This fit is plausible with the experimental data. The computed efficiencies compare well with the experimental data but the computed data indicate a weaker dependence of transformation efficiency on laser intensity.

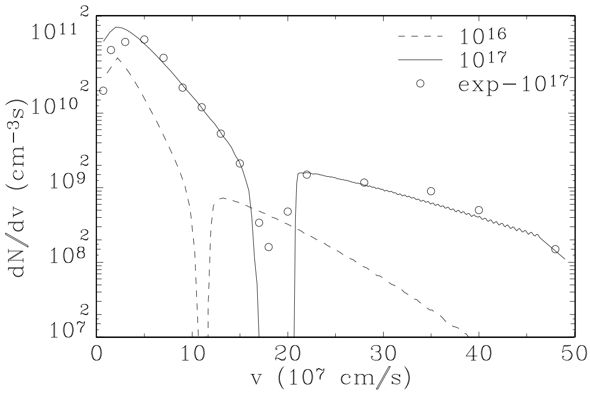

Fig. 3. Velocity spectrum of ions at the interaction of 1.5 ps FWHM Gaussian pulse of p-polarized Nd laser radiation incident at 45° on solid Al target for two values of laser intensity.

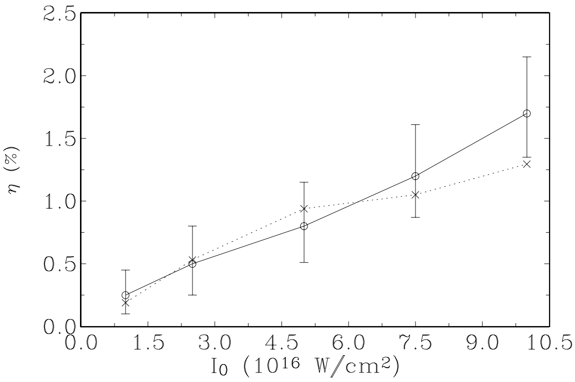

Fig. 4. Efficiency $\eta = I_2/I_0$ of laser energy transformation to SH emission from plasma versus peak laser intensity. P-polarized Gaussian 1.5 ps FWHM pulse of Nd-laser is assumed to be incident at 45° onto a solid aluminium target.

4. Conclusions

Self-contained 1D hydrodynamics model of interactions of short laser pulses with solid targets has been developed. Simulation results compare well with experiments in absorption efficiency, hot electron temperature, fast ion spectrum and SH emission intensity and spectra. Model may be used as a means of analysis of plasma dynamics and as an optimization tool for various output quantities, such as fast ion spectrum and x-ray yield.

Acknowledgements. Support by grant No. 202/97/1186 of the Grant Agency of the Czech Republic is gratefully acknowledged.

References

[1] P. Gibbon and E. Förster: Plasma Phys. Control. Fusion **38**, 769 (1996).

[2] J. Limpouch, L. Drska and M. Tagviashvili: in: Advances in Laser Interaction with Matter and Inertial Fusion. G. Velarde et al. eds., World Scientific 1997, p.621-624.

[3] N.E. Andreev, V.P. Silin and G.L. Stenchikov: ZhETF **78**, 1396 (1980).

[4] A.B. Gurevich and A.P. Mescherkin: ZhETF **80**, 1810 (1981).

[5] O. Peyrusse: Phys. Fluids **B4**, 2007 (1992).

[6] P. Gibbon and A.R. Bell: Phys. Rev. Letts. **68**, 1535 (1992)

[7] V.A. Komarov et al.: in: *Book of Abstracts, Laser Interactions and Related Plasma Phenomena*, Monterrey, U.S.A. 1997